

Stirring Effects and Phase-Dependent Inhomogeneity in Chemical Oscillations: The Belousov–Zhabotinsky Reaction in a CSTR

Fathei Ali and Michael Menzinger*

Department of Chemistry, University of Toronto, Toronto, Ontario M5S 3H6, Canada

Received: August 13, 1996; In Final Form: November 7, 1996[⊗]

The imperfect mixing of reactants in a continuously fed stirred tank reactor generates inhomogeneous perturbations that are responsible for stirring and mixing effects. Using a cellular mixing model and a kinetic model of the Belousov–Zhabotinsky reaction, we studied the statistical properties and dynamical consequences of the reactor inhomogeneities during limit cycle oscillations. Our key result—the time-dependent probability distribution—depends dramatically on oscillation phase: it is sharply peaked during the slow phase and broadens during the rapid phase of oscillation, where reaction is fast compared to mixing, and inhomogeneities and fluctuations are prominent. Observables are obtained from the probability distribution by appropriate averaging. We studied the stirring dependence of fluctuations and of the average oscillation amplitude and period, as well as the variance of these oscillation attributes.

A. Introduction

Inhomogeneity may drastically affect the rates and dynamics of imperfectly mixed, nonlinear chemical reactions,^{1,2} in particular those with chemical instabilities.^{3,4} In these reactions, inhomogeneous kinetics is manifest through so-called stirring effects: the dependence on stirring rate of steady state concentrations,^{1,5,6} of oscillation attributes,^{7–11} and of bifurcation points.^{5,6,8,10,12}

Fluid mixing proceeds by a stretching and folding process that gives rise to laminar structures with a wide distribution of length scales.^{13–15} While their detailed description has grown into an extensive literature in fluid dynamics and chemical and mechanical engineering, it is striking that this needs yet to be accompanied by similar studies incorporating chemical reactions.¹⁵ A different emphasis is placed in modeling studies of chemical instabilities^{16–19} where inhomogeneity is considered in a minimal, average way while reaction is treated in greater detail. While these approaches reproduce certain average aspects of the reactor response, much remains to be learned about the nature and role of the underlying inhomogeneities and the resulting fluctuations. In experiments, the statistical nature of the inhomogeneities shows up through concentration fluctuations^{5,9,20} and through irregular oscillation attributes such as amplitudes and periods.^{7,8,11} In oscillating systems one often finds that the fluctuation amplitude is a sensitive function of oscillation phase,^{8,9} reflecting a periodic variation of the system's response to external perturbations.

The objectives of this paper are to explore the statistical properties of the reactor inhomogeneities by adapting a cellular mixing (CM) model of the CSTR²¹ and to use the insights gained for interpreting qualitatively the dynamical consequences and stirring effects. A more quantitative application of the method to bistable systems will be reported elsewhere.⁴⁶ We employ a flow-Oregonator model of the Belousov–Zhabotinsky reaction and restrict ourselves to its oscillating regime. The CM model considers the CSTR as a collection of cells which are supplied, removed, and mixed by appropriate feeding and mixing protocols while each cell evolves like a homogeneous batch reactor. The state of the reactor is given by the concentration

vector of chemical species in every cell. From this, one readily constructs the time-dependent, multivariate probability distribution, the key result of this work. The probability distribution is a more informative platform than its average for understanding the CSTR dynamics and its stirring dependence. Macroscopic observables are obtained by appropriate averaging over the probability distribution. Specifically we address the relations between the probability distribution and the experimentally observable fluctuations, the irregularities of oscillation amplitude and period, and the dependence of these average oscillation attributes on mixing.

We find that the calculated probability distribution depends dramatically on oscillation phase. The broadening of the probability distribution that occurs during the phase of rapid autocatalytic explosion and the pronounced concentration fluctuations that have been observed in experiments with localized detection^{9,10,20} appear to be one and the same phenomenon. Given that the primary, mixing-induced perturbations arise independently of phase, the phase-dependent response of the system must reflect an intrinsic, local tendency of the limit cycle to process imposed perturbations. The rate with which perturbations from a limit cycle decay or grow is generally a sensitive function of phase,^{23,24} and globally stable limit cycles generally possess sensitive phases during which perturbations are amplified before they decay ultimately. Indeed, this tendency toward local instability is the source of chaotic dynamics in three dimensions, but it persists in two dimensions where topological constraints confine the system to limit cycles. Furthermore, the asymptotically contracting flow in phase space that characterizes dissipative dynamical systems does not always occur monotonically, and globally stable limit cycles may possess phases where phase volumes expand locally.²⁴ Our results show that the broadening of the probability distribution and the resulting growth of fluctuations are closely related to the local instability of the limit cycle, measured by the divergence $\text{div } f$ of the flow (1).

The probabilistic description of reactive systems is usually given by stochastic differential equations. Indeed, CM models may be recast in terms of stochastic differential equations^{21,25–27} that provide equivalent results. Stationary solutions of the Fokker–Planck equation for the Bonhoeffer–van der Pol

* Corresponding author.

[⊗] Abstract published in *Advance ACS Abstracts*, February 15, 1997.

model^{28,29} are in qualitative accord with the explicitly phase-dependent solutions reported here.

The Monte-Carlo version of Curl's cellular mixing model² was first described by Spielman and Levenspiel.³⁰ It is applied here to a CSTR with two separate, nonpremixed feedstreams and a two-variable kinetic system. The model assumes that the CSTR consists of N identical fluid parcels or cells labeled i , where each behaves as a homogeneous batch reactor. For the i th cell, the rate of change of the concentrations $c^i = (c_1^i, c_2^i)$ is given by

$$dc^i/dt = f(c^i) \quad (1)$$

The algorithm consists of the following steps: (1) The reactor is fed at intervals τ_f by replacing a pair of randomly chosen cells with two new cells with feedstream concentrations $(c_1^f, 0)$, $(0, c_2^f)$. The feeding interval τ_f is related to the residence time by $\tau_{res} = N\tau_f/2$. (2) Mixing is achieved at intervals τ_m by randomly picking a pair of cells and averaging (“coalescing and redispersing”) their concentrations. For any cell to undergo a mixing event, it takes on average $\tau_{mix} = N\tau_m/2$ time units, the characteristic mixing time of the reactor. (3) Between the periodic feeding and mixing events, the contents of each of the N cells evolves according to the rate law (1), which is integrated numerically.

The value of N was $N = 2598$. The resulting $2N$ rate equations were integrated on an SGI workstation using an implicit Euler scheme.³¹ One oscillation period required of the order of 1 h CPU time.

The dynamical state of the reactor is described by the $2N$ concentrations of species at time t . From this, a coarse-grained probability density $P(\bar{c}_1, \bar{c}_2; t)$ is constructed by sorting the cells into appropriately chosen concentration bins and equating the fraction of cells in the bin with central coordinates (\bar{c}_1, \bar{c}_2) to $P(\bar{c}_1, \bar{c}_2; t)$. Typically, a 100×100 grid of bins was used. These 3-D probability histograms are plotted in Figure 2a–c. An alternative scatter-plot representation of the same data is given in Figure 2d–f.

B. The Flow-Oregonator

The minimal kinetic model of the BZ system in a CSTR was obtained from the higher dimensional batch-Oregonator³³ by eliminating the rapidly varying reaction intermediates and retaining only those input species that are not bath species as dynamical variables,³⁴ and by adding the corresponding flow terms.³² The resulting two-variable flow-Oregonator is

$$\begin{aligned} dy/dt &= -k_1 h^2 a y - k_2 h x y + k_5 b f z + k_0 (y_0 - y) \\ dz/dt &= 2k_3 h a x - k_5 b z + k_0 (z_0 - z) \end{aligned} \quad (2)$$

where $x \equiv [\text{HBrO}_2]$, $y \equiv [\text{Br}^-]$, $z \equiv [\text{Ce(IV)}]$, $h \equiv [\text{H}^+]$, $a \equiv [\text{BrO}_3^-]$, $b \equiv [\text{MA}]$. The stoichiometric parameter f determines production of Br^- . The value of x is given by the equation of state, obtained by adiabatic elimination:

$$x = \frac{1}{4k_4} \left\{ -2k_2 h y + k_3 h a - k_0 + \sqrt{(k_3 h a - k_2 h y - k_0)^2 + 8k_1 k_4 h^2 a y} \right\} \quad (3)$$

The rate constants and parameter values, for which the simulations in Figures 1b,c, 2, 3, and 4 were done, are $k_1 = 2.0 \text{ M}^{-3} \text{ s}^{-1}$, $k_2 = 2.0 \times 10^8 \text{ M}^{-2} \text{ s}^{-1}$, $k_3 = 2.0 \times 10^3 \text{ M}^{-2} \text{ s}^{-1}$, $k_4 = 4.0 \times 10^8 \text{ M}^{-1} \text{ s}^{-1}$, $k_5 = 1.0 \text{ M}^{-1} \text{ s}^{-1}$, $k_0 = 0.0769823$, $f = 0.6$, $h = 1.0 \text{ M}$, $b = 20.0 \text{ M}$, $y_0 = 1 \times 10^{-5} \text{ M}$, and $z_0 = 1 \times$

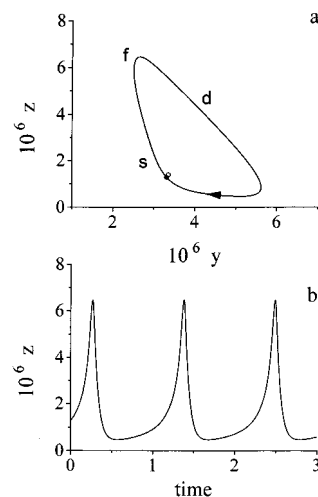


Figure 1. (a) One typical cycle in the phase plane. The open dot inside the cycle indicates the (unstable) fixed point. The solid dot on the cycle marks the reference phase $\phi = 0$. Labels s, f, d indicate the slow, fast, and decelerating phases. (b) Time series corresponding to part a.

10^{-5} M . The dimensioned model (2) may be directly related to experiments.

Figure 1a shows a limit cycle in the phase plane for the above parameter values. This limit cycle is nonuniform; that is, the rate of flow in phase space varies greatly, since the system spends most of the time in the “slow phase” near its unstable fixed point at low values of z and passes rapidly through its “fast phase” at high values of z . The corresponding time series $z(t)$ is Figure 1b. Most of the stochastic simulations were performed at this parameter value for computational convenience to prevent the limit cycle from being excessively stiff. Qualitatively similar results are also found elsewhere within the oscillatory domain. To illustrate the effect of stirring on the oscillation attributes, the calculations summarized in Figure 5 were done at the parameter value $k_0 = 0.1$ and $f = 0.5$, all others being the same as above.

C. Results and Discussion

Time-Dependent Probability Distribution. The probability distribution $P(y,z;t)$ completely describes the state of the system as a function of time. Its first moments are the mean concentrations, and the second moments are the variances, related to the mean fluctuation amplitudes. First, we show how the probability distribution evolves along a typical cycle as a function of time. We express time in terms of the phase ϕ , defined by $\phi = t/T$, where T is the oscillation period. Figure 2a,b,c illustrates the evolution of $P(y,z;t)$ through three snapshots during the slow, fast, and decelerating phases, respectively. To appreciate the pronounced phase-dependence or “breathing motion” of the probability distribution, the different scales of the panels should be noted. During the slow phase, the probability distribution is sharply localized. As the system passes through its fast phase, it broadens dramatically. This means that the reactor is relatively homogeneous during the slow phase and that it becomes very inhomogeneous during its fast phase. An alternative representation is given by the scatter plots Figure 2d,e,f. The solid line in the scatter plots represents the mean concentration during a cycle. To quantify the degree of inhomogeneity of the reactor, we use here the mean deviation from the average

$$\sigma_N = \frac{1}{N} \sum_{i=1}^N \sqrt{(y_i - \langle y \rangle)^2 + (z_i - \langle z \rangle)^2} \quad (4)$$

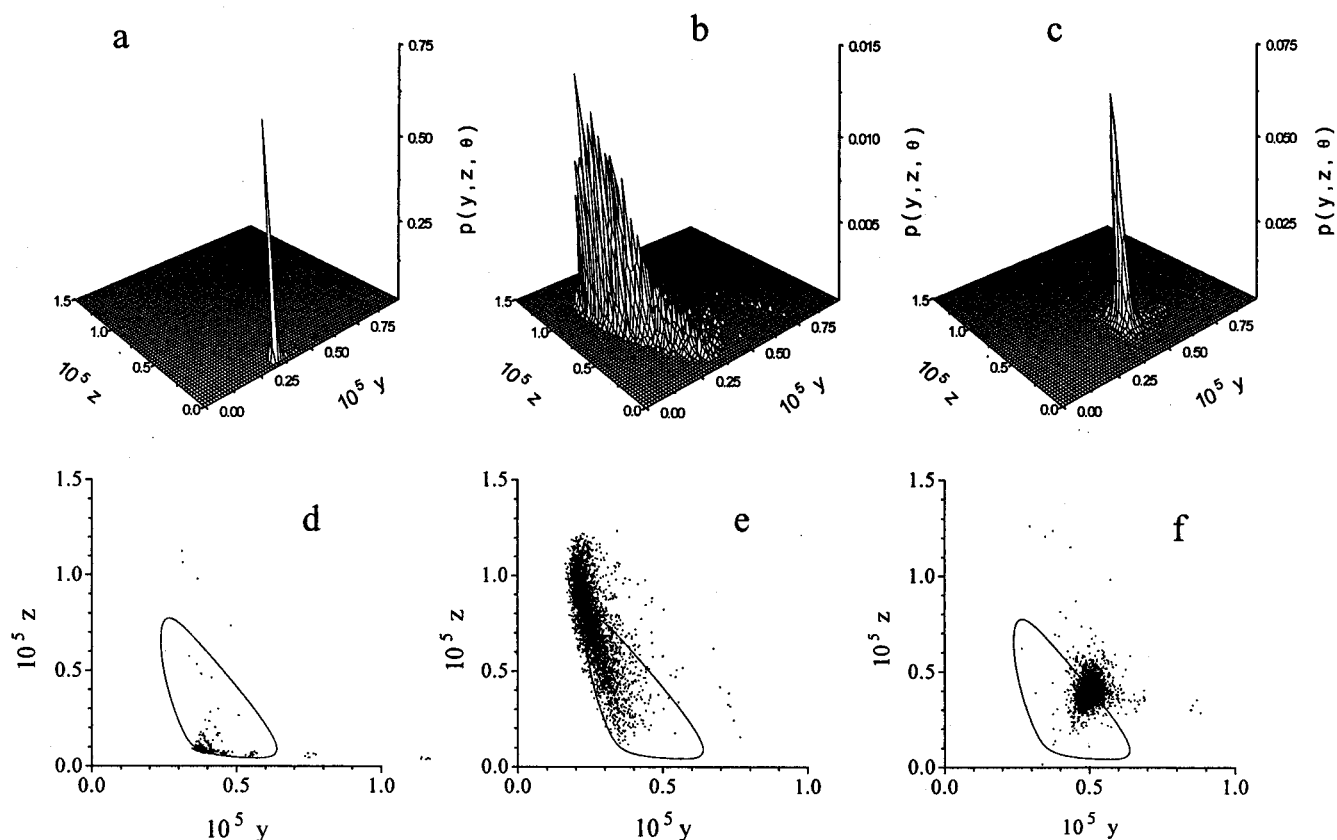


Figure 2. Calculated probability distribution, $P(y, z; t)$ for three phases (a, b, c) on the cycle. Parameters are $N = 2598$, $\tau_{\text{mix}} = 0.01299$, $\tau_{\text{res}} = 0.07698$ (corresponding to k_0 in Figure 1b). (d, e, f) Same data as a, b, c represented as scatter plots. One average cycle is shown by the orbits.

This may also be viewed as a measure of the fluctuation amplitude, although more appropriate definitions may be adopted, depending on the nature of the detector (e.g. light absorption or electrochemical response to a specific ion). This issue is not pursued here. How can physical experiments provide a measure of the reactor inhomogeneity? If it were possible to monitor a variable on a sufficiently fine spatial scale, corresponding to a single cell, one would obtain a time series whose fluctuations accurately reflect the probability distribution in one direction. In reality, detection usually introduces some spatial and temporal averaging, and the magnitude of the resulting fluctuations is correspondingly reduced. This is illustrated by Figure 3a,b. Panel b represents the noisy “microelectrode” signal $\langle z(\phi) \rangle_{10}$ by the average over 10 randomly chosen cells. The fluctuations are most pronounced at the peak of the signal (cf. Figure 1b) where the probability distribution (Figure 2b,e) has reached its maximum spread. The local fluctuation amplitude is also a measure of the width of the probability distribution. Panel a represents a “macroelectrode” signal given by the ensemble average $\langle z(\phi) \rangle_N$ over the entire reactor: fluctuations are drastically reduced. Thus, by monitoring the system on a small spatial scale^{8,9,20} and analyzing the local fluctuation amplitude, one may obtain a measure of the width of the probability distribution.

Figure 3c illustrates the pronounced phase-dependence of the fluctuations. It demonstrates that the system’s response to constant input noise is an equally pronounced function of oscillation phase. To interpret this observation, recall^{23,24,28,35} that the response of an oscillator to perturbations of its dynamical variables is related to its “local stability”, i.e. to the local rate of decay or growth of the perturbation to or from the limit cycle. It is known^{23,24} that globally stable limit cycles generally possess locally unstable phases during which perturbations from the cycle grow, before they ultimately decay. Furthermore, regions

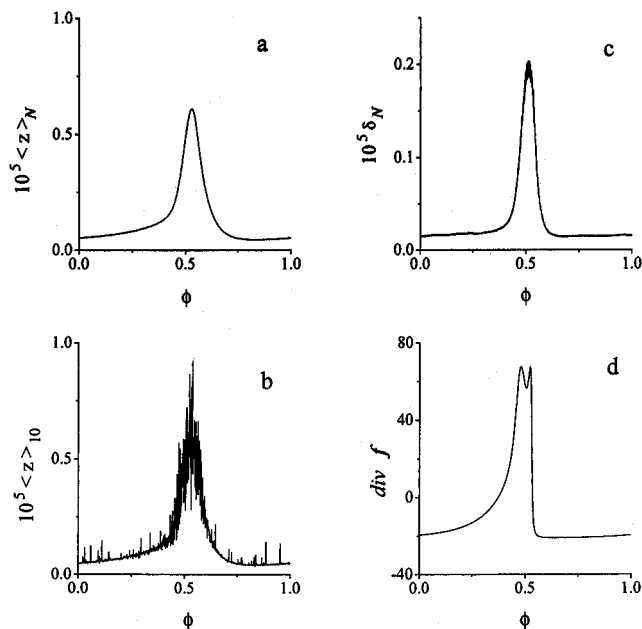


Figure 3. Responses of (a) “macroelectrode” signal, $\langle z \rangle_N$ and (b) “microelectrode” signal, $\langle z \rangle_{10}$. The comparison between (c) the degree of inhomogeneity or fluctuation amplitude $\delta(\phi)$ and (d) the divergence of the flow $\text{div}(f)$ evaluated along the stochastic limit cycle illustrates the role of local stability in the evolution of fluctuations.

in phase space may exist where volumes expand locally,²⁴ before they contract eventually, as is required for dissipative systems. The rate of change of volume elements in phase space is given by the divergence $\text{div}(f)$ of the flow (equal to the trace of the linear stability matrix) of the dynamical system (1). A negative divergence corresponds to contraction (dissipation), and a positive divergence to expansion. To show that the dramatic

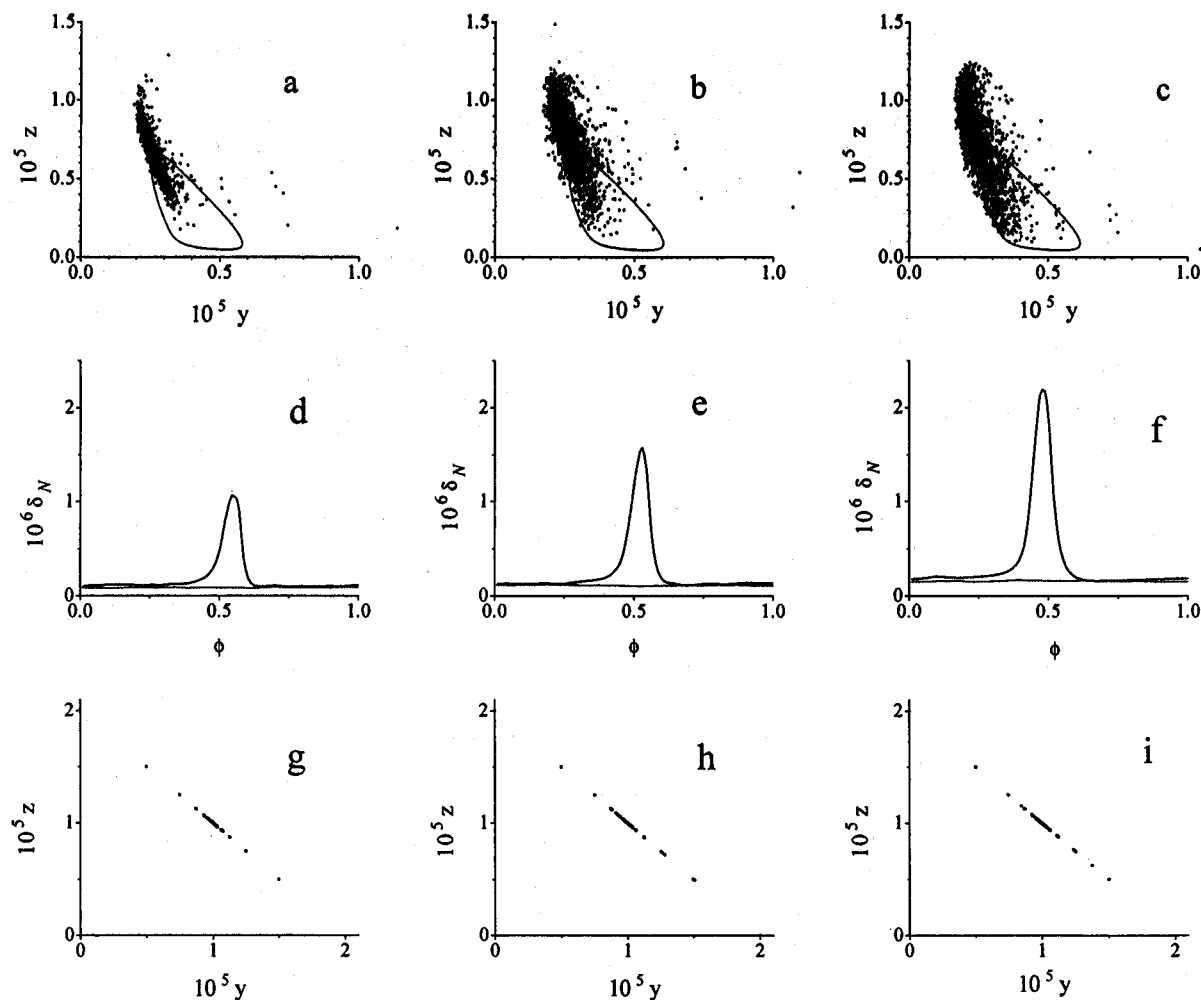


Figure 4. (a, b, c) Effect of mixing on the probability distribution at the same, fast phase. (a) $\tau_{\text{mix}} = 0.00812$, (b) $\tau_{\text{mix}} = 0.01083$, (c) $\tau_{\text{mix}} = 0.01624$. (d, e, f) Bell-shaped curves showing the corresponding average absolute deviations $\delta(\phi)$ of the probability distributions over one cycle. (g, h, i) Nonreactive probability distributions for the same parameter values as in a, b, c. The intercepts on the axes are the feed concentrations y_0 , z_0 .

expansion of the ensemble of phase points early in the rapid phase in Figure 2 is associated with a positive value of the divergence, we compare the computed fluctuation amplitude, Figure 3c, with the divergence of the flow, Figure 3d, of the deterministic model (2). The similarity of the two plots shows that the local instability of the cycle plays a major role in the evolution of fluctuations and of the probability distribution.

Stirring Effects. It is intuitively clear that the reactor becomes more inhomogeneous as mixing is slowed down. Figure 4a,b,c illustrates this broadening of the probability distribution with decreasing the mixing rate at the same, fast phase. The width $\delta(\phi)$ of the distribution is most sensitive to stirring during its most diffuse, rapid phase (Figure 4d,e,f). Indeed, all stirring effects that were surveyed in the Introduction may be viewed in the light of such changes of the probability distribution.

The evolution of the probability distribution may be divided into two conceptual stages: first comes the nonreactive turbulent mixing that gives rise to turbulent eddies.^{13,14} This is followed by the chemical transformation of the turbulent eddies. To make this conceptual picture explicit, we have calculated in Figure 4g,h,i the probability distribution corresponding to nonreactive mixing. Mass conservation constrains the unreactive cells to the straight line connecting the feed concentrations. The width $\delta(t)$ of these one-dimensional distributions, given by the thin horizontal lines at the bottom of Figure 4d,e,f, increases slightly with τ_{mix} . The essential point to be noted is that despite the

very different appearances of the reactive and nonreactive distributions during the slow phase of the reaction, the corresponding widths δ are very close to each other. This suggests that mixing, rather than chemical relaxation, determines the width of the probability distribution when reaction is slow. Chemical reaction plays a key role in the growth and decay of fluctuations only when its time scale is on the order of or shorter than the mixing time. This is the case during the fast, autocatalytic phase of the cycle: mixing can then no longer keep up with chemical relaxation and the reactor inhomogeneity becomes large.

Next we address in Figure 5 the experimentally well-known deviation of limit cycle oscillations from perfect periodicity.^{8,36,37} Time series and phase plane plots are given for slow mixing in Figure 5a,b and for rapid mixing in Figure 5c,d. Obviously, the probability density and the averages derived from it are fluctuating quantities. The irregular amplitude at the slow mixing rate and the jittery cycle in the phase plane are a consequence of the broad probability distribution during the fast oscillation phase. As the distribution narrows at the higher mixing rate, the irregularity of the amplitude decreases. The period fluctuates also, but to a lesser degree than the amplitude.

Most prominent in Figure 5 is the effect of mixing on the average oscillation attributes. As the mixing rate is reduced, the limit cycle shrinks and the period decreases. τ_{mix} indicates the presence of a supercritical Hopf bifurcation. However the amplitude does not vanish completely since the inhomogeneities

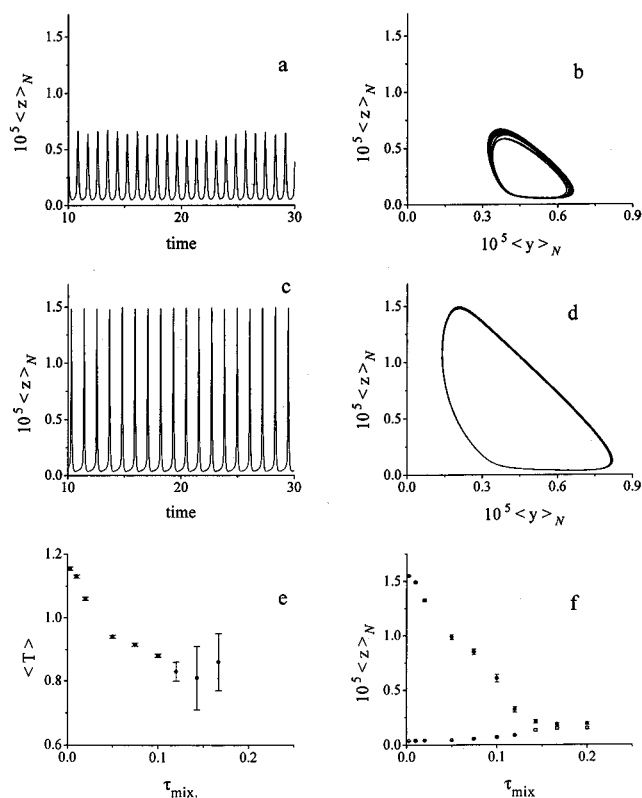


Figure 5. Effect of mixing on limit cycle attributes: (a) time series and (b) phase plot at slow mixing ($\tau_{\text{mix}} = 0.1$). (c, d) The same at rapid mixing ($\tau_{\text{mix}} = 0.01$). (e) Effect on the average period. (f) Effect on oscillation amplitude.

maintain the system in a state of noise-induced, low-amplitude oscillations long after the passage of the Hopf point.³⁸ The precise location of the Hopf point might be obtained through an additional analysis.³⁸ The average oscillation period T (Figure 5e) decreases over the same range of mixing rates and finally levels out, while its variance suddenly increases sharply, signaling the region of bifurcation and the noise-induced state beyond it. Experiments in the batch-BZ system^{9,39,40} and in the chlorite–iodide system in a CSTR^{8,10} have shown similar trends of decreased amplitude and period at reduced stirring rates. This was explained^{9,41} by the help that external noise provides in skipping over the slow portion of the cycle when the system spends a long time in one part of the cycle (e.g. Figure 1b). However, this trend is not generic, and the opposite stirring effect—a slowing-down of oscillations at decreased stirring—has been reported occasionally.^{37,42,43}

D. Conclusion

The key result of this paper is the statistical description of limit cycle oscillations in a CSTR that is provided by the explicitly calculated time-dependent probability distribution. Formally related are the stationary and time-dependent solutions of the multivariate master equation^{44,45} that describes the dynamics of internal fluctuations. While internal fluctuations are important in systems with low levels of external noise, extrinsic noise often dominates. The CSTR is such a system in which the external noise source is well understood, intense, and readily detectable. The present results illustrate the close relationship that exists between the moments of the probability distribution, the fluctuation amplitude, and the local stability properties of limit cycles. They provide a guide for extracting information on the local stability of the cycle from suitably recorded experimental time series.

The well-known irregularities of limit cycle oscillations may be readily understood in light of the probability distribution function. The dependence of the probability distribution on mixing rate provides some insight into the stirring effects, although further work is required to fully understand the connection between inhomogeneity and the oscillation attributes. The technique described and applied here to limit cycle oscillations has been used to provide more quantitative information on the stirring effects on steady states and bistability limits.⁴⁶ A theoretical interpretation, based on stochastic differential equations, has been developed.³⁸

The two-variable flow-Oregonator was used here for computational convenience. However, the use of reduced kinetic models to describe stirring effects may not be quite appropriate since the fastest steps, whose reactants are often adiabatically eliminated, will be the first to compete effectively with the mixing process and give rise to the kind of stirring effects that we address in this paper. In other words, in reactions with fast steps (e.g. autocatalytic explosion), incomplete mixing may effectively “awaken” the hidden degrees of freedom. Evidence for such an effect occurs in the minimal bromate oscillator,⁶ where stirring affects the bistability hysteresis in a qualitatively different way from the classical Belousov–Zhabotinsky reaction.⁴⁷ We have argued⁴⁷ that this difference in stirring effects reflects the difference of the number of effective degrees of freedom in both systems. This issue goes however beyond the present paper and requires further work.

As used here, the CM model does not contain any spatial information and disregards the anisotropy of the CSTR.¹⁵ The anisotropy of the turbulent reactive flow is related to macroscopic concentration gradients⁴⁸ in the CSTR. However, the CM model may be adapted to describe such spatial effects by attaching spatial meaning and a varying mixing intensity to the cell indices.

Acknowledgment. This work is supported by the NSERC of Canada.

References and Notes

- Villermaux, J. *Rev. Chem. Eng.* **1991**, 7, 51.
- Bourne, J. R.; Rys, P.; Suter, K. *Chem. Eng. Sci.* **1977**, 32, 711.
- Villermaux, J. In *Spatial Inhomogeneities and Transient Behavior in Chemical Kinetics*; Baras, G., Borckmans, F., Scott, P., Gray, S. K., Nicolis, P., Eds.; Manchester University Press: Manchester, U.K., 1990.
- Epstein, I. R. *Nature* **1995**, 374, 321.
- Roux, J. C.; DeKepper, P.; Boissonade, J. *Phys. Lett.* **1983**, 97A, 168.
- Dutt, A. K.; Menzinger, M. *J. Phys. Chem.* **1990**, 94, 4867.
- Smoes, M. L. *J. Chem. Phys.* **1979**, 71, 4669.
- Menzinger, M.; Giraudi, A. *J. Phys. Chem.* **1987**, 91, 4391.
- Menzinger, M.; Jankowski, P. *J. Phys. Chem.* **1986**, 90, 1217.
- Luo, Y.; Epstein, I. R. *J. Chem. Phys.* **1986**, 85, 5733.
- Nagyal, I.; Epstein, I. R. *J. Phys. Chem.* **1986**, 90, 6285.
- Boukalouch, M.; Boissonade, J.; DeKepper, P. *J. Chim. Phys. (Paris)* **1987**, 84, 1353.
- Kolmogorov, A. N. *C. R. Akad. Nauk* **1944**, 30, 301.
- Ottino, J. M. *The Kinematics of Mixing: Stretching, Chaos and Transport*; Cambridge Univ. Press: Cambridge, 1989.
- Ottino, J. M. *Chem. Eng. Sci.* **1994**, 49, 4005.
- Kumpinski, E.; Epstein, I. R. *J. Chem. Phys.* **1985**, 62, 53.
- Ali, F.; Menzinger, M. *J. Phys. Chem.* **1991**, 95, 6408.
- Fox, R. O.; Villermaux, J. *Chem. Eng. Sci.* **1990**, 45, 2857.
- Puhl, A.; Nicolis, G. *J. Chem. Phys.* **1987**, 87, 1070.
- Menzinger, M.; Jankowski, P. *J. Phys. Chem.* **1990**, 94, 4123.
- Curl, R. L. *AIChE J.* **1963**, 9, 175.
- Ali, F. *Stirring and mixing effects in chemical instabilities: The chlorite-iodide reaction*. Master’s Thesis, University of Toronto, 1992.
- Nese, J. M. *Physica D* **1989**, 35, 237.
- Ali, F.; Menzinger, M. On the local (in)stability of limit cycles, in preparation.
- Evangelista, J. J.; Katz, S.; Shinnar, R. *AIChE J.* **1969**, 15, 843.
- Horsthemke, W.; Hannon, L. *J. Chem. Phys.* **1984**, 81, 4363.
- Hannon, L.; Horsthemke, W. *J. Chem. Phys.* **1987**, 86, 140.

- (28) Kurrer, C.; Schulten, K. *Physica D* **1991**, *50*, 311.
(29) Treutlein, H.; Schulten, K. *Eur. Biophys. J.* **1986**, *13*, 355.
(30) Spielman, L. A.; Levenspiel, O. *Chem. Eng. Sci.* **1965**, *20*, 247.
(31) Hairer, E.; Wanner, G. *Solving Ordinary Differential Equations II. Stiff and Differential-Algebraic Problems*; Springer-Verlag: Berlin, 1991.
(32) Gáspár, V.; Showalter, K. *J. Chem. Phys.* **1988**, *88*, 778.
(33) Field, R. J.; Noyes, R. M. *J. Chem. Phys.* **1974**, *60*, 1877.
(34) Bar-Eli, K.; Field, R. J. *J. Phys. Chem.* **1990**, *94*, 3660.
(35) Keizer, J.; Fox, R. F.; Wagner, J. *Phys. Lett. A* **1993**, *175*, 17.
(36) Resch, P.; Münster, A. F.; Schneider, F. W. *J. Phys. Chem.* **1991**, *95*, 6275.
(37) Dutt, A. K.; Müller, S. C. *J. Phys. Chem.* **1993**, *97*, 10059.
(38) Strizhak, P.; Menzinger, M. *J. Phys. Chem.*, in press.
(39) Farage, U. J.; Jancic, D. *Chimia* **1981**, *35*, 289.
(40) Ruoff, P. *Chem. Phys. Lett.* **1982**, *90*, 76.
(41) Rappel, W. J.; Strogatz, S. H. *Phys. Rev. E* **1994**, *50*, 3249.
(42) Noszticzius, Z.; Bondár, Z.; Garanzegi, L.; Wittman, M. *J. Phys. Chem.* **1991**, *95*, 6675.
(43) Weissenberger, S. Diploma Thesis, University of Würzburg, 1993.
(44) Turner, J. W. *Dynamics of Synergetic Systems*; Haken, H., Ed.; Springer Verlag: Berlin, 1980.
(45) Nicolis, G.; Malek-Mansour, M. *Progr. Theor. Phys. Suppl.* **1978**, *64*, 249–268.
(46) Ali, F.; Strizhak, P.; Menzinger, M. In preparation.
(47) Strizhak, P.; Menzinger, M. *J. Phys. Chem.* **1996**, *100*, 19182.
(48) Menzinger, M.; Dutt, A. K. *J. Phys. Chem.* **1990**, *94*, 4510.